Journal of Materials Science and Chemical Engineering, 2026, 14(11), 108-119
https://www.scirp.org/journal/msce
ISSN Online: 2327-6053
ISSN Print: 2327-6045

Design of an Inquiry-Based Comprehensive Experiment for Hydrothermal Preparation of RGO/MnO_2 Composites under the Background of Emerging Engineering Education

Ao Chen[1], Jie Zhang[1], Li Lian[2], Huiyuan Zhang[2]*

[1]Guangzhou Railway Polytechnic, Guangzhou, China
[2]Hebei Key Laboratory of Hazardous Chemicals Safety and Control Technology, School of Chemical Safety, University of Emergency Management, Langfang, China
Email: *zhanghy@ncist.edu.cn

How to cite this paper: Chen, A., Zhang, H.Y., Lian, L. and Zhang, J. (2026) Design of an Inquiry-Based Comprehensive Experiment for Hydrothermal Preparation of RGO/MnO_2 Composites under the Background of Emerging Engineering Education. *Journal of Materials Science and Chemical Engineering*, **14**, 108-119.
https://doi.org/10.4236/msce.2026.1411007

Received: October 29, 2026
Accepted: November 23, 2026
Published: November 26, 2026

Copyright © 2026 by author(s) and Scientific Research Publishing Inc.
This work is licensed under the Creative Commons Attribution International License (CC BY 4.0).
http://creativecommons.org/licenses/by/4.0/
Open Access

Abstract

In response to the talent-training requirements of integrating scientific research with teaching under Emerging Engineering Education 2.0, this study transforms the scientific research topic of preparing RGO/MnO_2 composites for supercapacitors into an inquiry-based comprehensive experiment for students majoring in new-energy-related materials. Graphene oxide (GO) was synthesized via the modified Hummers method, and reduced graphene oxide (RGO) was further obtained by liquid-phase reduction using L-ascorbic acid. RGO/MnO_2 composites with feed mass ratios of 1:1, 2:1 and 3:1 were hydrothermally fabricated using potassium permanganate as the manganese source. Multi-dimensional material characterizations including FE-SEM-EDS, FTIR, BET and contact-angle measurements were carried out to investigate the effects of manganese-source dosage on the micromorphology, elemental composition, surface wettability and specific surface area of the as-prepared composites. The experimental results show that the wettability and specific surface area are improved after compounding RGO with MnO_2. Nevertheless, excessive manganese-source dosage triggers severe agglomeration of MnO_2 particles and increases the ion-diffusion resistance of the electrolyte. This experiment integrates multidisciplinary knowledge covering inorganic-material synthesis, large-scale-instrument characterization and data analysis. It trains students to develop the scientific-research thinking of controlling variables and establishes the logic of cross-verification among multiple characterization methods. It can serve as a referential experimental case for inquiry-oriented teaching in the energy-storage field under Emerging Engineering Education.

Keywords

Emerging Engineering Education, Inquiry-Based Experiment, Reduced Graphene Oxide, Manganese Dioxide, Material Characterization

1. Introduction

With the integrated development of education, science-technology and talent cultivation, Emerging Engineering Education 2.0 emphasizes interdisciplinary integration, scenario-oriented teaching and industrial-oriented achievement transformation, which puts forward higher requirements for the practical capabilities and innovation competence of students majoring in materials and chemical engineering [1] [2]. Traditional verification-based experiments adopt fixed workflows, where students merely follow preset procedures to operate equipment. Such teaching mode lacks training in variable exploration, phenomenon interpretation and mechanism analysis, resulting in the disconnection between scientific research and classroom teaching [3]. Transforming mature scientific-research systems in the field of new-energy storage into inquiry-oriented teaching experiments, and guiding students to independently complete material preparation, multi-characterization testing, data analysis and mechanism discussion, is an effective way to implement the educational concept of integrating scientific research with teaching [4].

As a typical new-energy-storage device, supercapacitors exhibit prominent advantages including high power density, fast charge-discharge rate and long cycle life. Reduced graphene oxide (RGO) possesses two-dimensional wrinkled sheet structures and excellent electrical conductivity, which mainly contributes to electric-double-layer capacitance. Manganese dioxide (MnO_2) is abundant in reserves and low-cost, and can provide abundant pseudocapacitive active sites. However, its intrinsically poor electrical conductivity easily leads to nanoparticle agglomeration. Hydrothermal *in-situ* compounding of RGO and MnO_2 can construct continuous conductive networks relying on RGO, while MnO_2 provides Faradaic redox reaction sites. The synergistic complementarity of the two components improves the energy-storage performance of electrodes [5]-[7].

In this paper, the research topic of RGO/MnO_2 composites is redesigned into an inquiry-based comprehensive teaching experiment. Students prepare GO by the modified Hummers method and obtain RGO via L-ascorbic-acid reduction. RGO/MnO_2 composite powders with different mass ratios are hydrothermally synthesized by adjusting the dosage of potassium permanganate. A series of characterizations including FE-SEM-EDS, FTIR, BET and contact-angle measurements, are performed to explore the influences of feed ratios on micromorphology, wettability and specific surface area. Focusing on the module of "material synthesis-structural characterization", this experiment covers nanomaterial preparation, large-instrument operation and experimental-data analysis. It helps stu-

dents understand the energy-storage mechanism of supercapacitors, establish the "preparation-structure-performance" logical correlation, and cultivate their scientific-inquiry capability with controlled-variable thinking.

2. Experiments

2.1. Experimental Purposes

On the one hand, students are expected to understand the preparation principles of supercapacitor electrode materials, master the experimental procedures of preparing GO by the modified Hummers method, reducing GO into RGO with L-ascorbic acid, and hydrothermally synthesizing RGO/MnO_2 composites. They should also explore how the manganese-source dosage affects the micromorphology, surface wettability and specific surface area of composite electrodes. On the other hand, students are required to independently propose a hypothesis about the relationship between $KMnO_4$ dosage and composite microstructure, select evaluation indicators (morphology, element distribution, wettability and BET specific surface area) to compare samples, and analyze the advantages and limitations of each characterization method. These open-ended tasks are designed to realize inquiry-based learning rather than simple cookbook verification.

2.2. Experimental Raw Materials and Instruments

2.2.1. Raw Materials

Graphite powder (≥99.8%, Shanghai Aladdin Biochemical Technology Co., Ltd.); potassium permanganate (≥99.5%, Tianjin Yongda Chemical Reagent Co., Ltd.); concentrated sulfuric acid (98%, Tianjin Yongda Chemical Reagent Co., Ltd.); hydrogen peroxide (30%, Tianjin Yongda Chemical Reagent Co., Ltd.); L-ascorbic acid (≥99%, Tianjin Yongda Chemical Reagent Co., Ltd.); ammonia water (25%, Tianjin Yongda Chemical Reagent Co., Ltd.); hydrochloric acid (36% - 38%, Tianjin Damao Chemical Factory); polyvinylidene fluoride (PVDF, SOLVAY); N-methyl-2-pyrrolidone (NMP, Shanghai Aladdin); acetylene black; nickel foam; sodium chloride; absolute ethanol; laboratory-prepared deionized water.

Safety precautions: Concentrated sulfuric acid and potassium permanganate are highly corrosive and oxidizing. All manipulations should be performed in a fume hood. The loading capacity of the hydrothermal autoclave must be strictly regulated, and the autoclave can only be opened after natural cooling to room temperature. NMP is an irritant, and rubber gloves are required during handling. Manganese-containing waste solutions should be collected separately for centralized disposal instead of direct discharge into drains.

2.2.2. Instruments

METTLER-TOLEDO electronic analytical balance; MSH280-Pro magnetic stirrer; LD5-2A high-speed desktop centrifuge; FD-1A-50 freeze-dryer; DZF-6020B vacuum drying oven; DF-101S thermostatic-heating magnetic stirrer; GeminiSEM·300 field-emission scanning electron microscope; ALPHA-II Fourier-transform infrared spectrometer; BSD-660 specific-surface-area analyzer; XGC-

AMB3 contact-angle tester.

2.3. Experimental Procedures

2.3.1. Preparation of GO, RGO and RGO/MnO_2 Composites

1) Synthesis of graphene oxide (GO)

Under an ice-water-bath condition, 1.0 g graphite powder was added into 30 mL concentrated sulfuric acid under stirring. 2.0 g $KMnO_4$ was added portion-wise, and the mixture was stirred for 2 h with the temperature controlled below 10˚C. Afterwards, the system was heated to 35˚C for 30 min water-bath reaction. Deionized water was added for dilution, and H_2O_2 was drop-wise added to terminate oxidation, yielding bright-yellow GO suspension. The suspension was centrifugally washed with hydrochloric acid and deionized water until pH reached 6.5 - 7.0, and GO slurry was collected.

2) Synthesis of reduced graphene oxide (RGO)

GO was formulated into 1 mg/mL aqueous dispersion and ultrasonically exfoliated in an ice-water bath for 30 min. Ammonia water was used to adjust pH to 9.0 - 10.0. L-ascorbic acid was added at a mass ratio of L-ascorbic acid:GO = 8:1, and reflux reaction was carried out at 90˚C - 95˚C for 3 h. After centrifugal washing, the product was pre-frozen at 80˚C and freeze-dried to obtain fluffy RGO powder.

3) Hydrothermal synthesis of RGO/MnO_2 composites and electrode-slice fabrication.

RGO was fixed at 0.2 g, and $KMnO_4$ dosages of 0.2 g, 0.4 g and 0.6 g were set for three groups of samples. 0.2 g freeze-dried RGO powder was dispersed in 20 mL deionized water and ultrasonically treated in ice-water bath at 500 W for 30 min. Corresponding amounts of $KMnO_4$ were added, followed by another 15 min ice-bath sonication. The mixed dispersion was transferred into a 50 mL PTFE-lined hydrothermal autoclave, supplemented with deionized water up to 80 % of autoclave volume, stirred and sealed. Hydrothermal reaction proceeded at 120˚C for 12 h. After natural cooling to room temperature, precipitates were collected by centrifugation at 8000 r/min for 10 min. The precipitates were washed three times with deionized water and once with absolute ethanol (centrifugation at 8000 r/min for 10 min after each washing step) to remove residual potassium salts and unreacted precursors. The precipitates were vacuum-dried at 60 ˚C under 0.08 MPa for 12 h to acquire RGO/MnO_2 composite powders.

Composite powder, acetylene black and PVDF were weighed at a mass ratio of 8:1:1 with total mass of 10 mg (8 mg composite powder, 1 mg acetylene black, 1 mg PVDF). The mixtures were ground in an agate mortar with appropriate NMP for 30 min to form homogeneous viscous electrode slurry. The slurry was uniformly coated onto pre-treated nickel-foam substrates with a coating area of 1 cm × 1 cm and coating thickness of approximately 50 μm. The coated electrode slices were vacuum-dried at 80˚C for 6 h to remove NMP solvent.

2.3.2. Structural and Morphological Characterizations

Field-emission scanning electron microscopy (FE-SEM), Fourier-transform in-

frared spectroscopy (FTIR), contact-angle measurement and BET nitrogen-adsorption-desorption test were adopted to characterize micromorphology and surface properties. Gold sputtering was performed for FE-SEM samples before testing. Acceleration voltage and magnification were adjusted to observe morphology and dispersion status. FTIR spectra were recorded in the wavenumber range of 4500 - 400 cm^{-1} with a resolution of 4 cm^{-1}. Electrode slices were fixed on the sample stage for contact-angle measurement, and electrolyte droplets were applied to evaluate surface wettability. The BSD-660 physical-adsorption instrument was used for BET measurement. Vacuum degassing was conducted prior to N_2 adsorption-desorption tests to obtain specific-surface-area and pore-structure parameters. The detailed parameters are listed as follows: pre-freezing temperature: −80˚C; BET degassing: 120˚C, 6 h; contact angle: droplet volume 5 μL, tested at 3 s after droplet deposition, each sample was measured at 5 different positions.

3. Results and Discussion

These multi-characterization techniques not only analyze material structure-performance relationships, but also serve teaching purposes. They help students understand the applicable scenarios of different large-scale instruments, build the scientific idea that "single characterization has limitations and cross-verification from multiple characterizations is required", learn to extract valid experimental information from spectra and tables, and train their capabilities in data analysis and logical deduction.

3.1. Morphological Analysis of Composites

FE-SEM coupled with EDS was employed to characterize the micromorphology and elemental distribution of RGO and RGO/MnO_2 composites with different feed ratios, so as to explore the influence of manganese-source dosage on microstructure and particle dispersion. For student learning, SEM cultivates the observation of micro-phenomena including two-dimensional sheets, nanoparticles and particle agglomeration from microscale perspectives. EDS enables students to judge component variation from elemental information and realize the inherent limitations of EDS, avoiding hasty conclusions derived merely from single spectra.

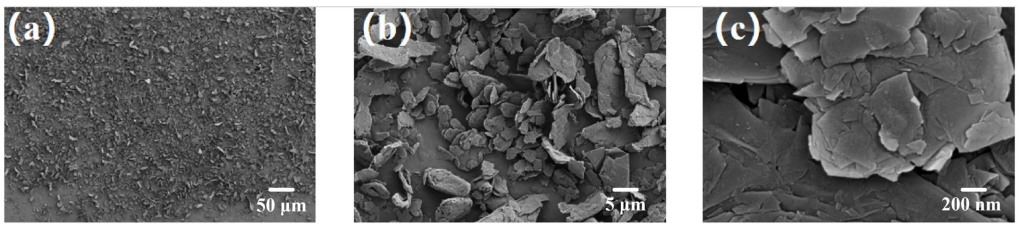

Figure 1. SEM images of graphene at different magnifications: (a) 50 μm; (b) 5 μm; (c) 200 nm.

Figure 1 presents SEM micrographs of pure RGO at different magnifications. At low magnification (Figure 1(a)), RGO shows irregular stacking and rough surfaces, and two-dimensional sheets agglomerate to some extent after drying. Me-

dium-magnification image (Figure 1(b)) displays uneven sheets interlaced with each other, and inter-sheet gaps form pores for electron transport. Typical wrinkled layered graphene structures can be observed in the high-magnification image (Figure 1(c)). The wrinkled RGO sheets act as conductive skeletons for MnO_2 growth to guarantee electron conduction. Nevertheless, π-π interaction induces sheet stacking, partial pores are covered, which hinders electrolyte-ion diffusion to a certain degree.

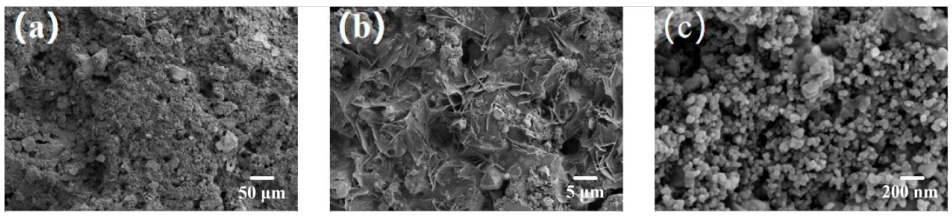

Figure 2. SEM images of RGO/MnO_2-1:1 composite at different magnifications: (a) 50 μm; (b) 5 μm; (c) 200 nm.

Table 1. Elemental composition of RGO/MnO_2-1:1 composite.

Element	Weight %	Atomic %
C	99.88	99.97
Mn	0.12	0.03
Total	100.00	100.00

Figure 2 shows SEM and EDS results for RGO/MnO_2-1:1 composite. At low magnification (Figure 2(a)), the sample exhibits rough porous stacking structures. The medium-magnification image (Figure 2(b)) shows a small quantity of nanoparticles attached to wrinkled RGO sheets. High-magnification observation (Figure 2(c)) confirms *in-situ* generation of MnO_2 nanoparticles on RGO sheets with slight local agglomeration. According to Table 1, carbon dominates the elemental composition while Mn mass fraction is only 0.12 %, indicating low MnO_2 loading (The Mn and C mass fractions are local-region elemental estimates, which cannot fully represent the bulk composition of the composite material). No oxygen signal is detected in this EDS result. EDS can merely identify elemental species rather than chemical bonds or crystal phases. Hence FTIR results are required for further corroboration. This case guides students to realize that multiple characterizations must be combined for comprehensive analysis.

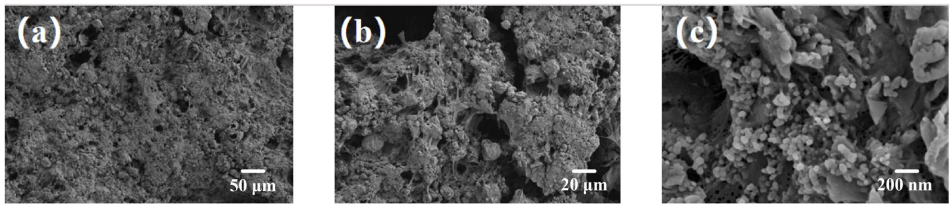

Figure 3. SEM images of RGO/MnO_2-2:1 composite at different magnifications: (a) 50 μm; (b) 20 μm; (c) 200 nm.

Table 2. Elemental composition of RGO/MnO_2-2:1 composite.

Element	Weight %	Atomic %
C	69.81	95.36
Mn	30.19	4.64
Total	100.00	100.00

Figure 3 corresponds to RGO/MnO_2-2:1 composite. Loose porous block-like stacking with abundant pores can be seen in **Figure 3(a)**. Wrinkled RGO sheets interlace with each other and are decorated by massive nanoparticles (**Figure 3(b)**, **Figure 3(c)**). Compared with the 1:1 sample, the number of MnO_2 nanoparticles increases significantly. **Table 2** demonstrates the rise of Mn mass fraction up to 30.19 %, verifying that higher $KMnO_4$ dosage improves MnO_2 loading. Continuous RGO sheets maintain electrical conductivity, and MnO_2 nanoparticles provide pseudocapacitive active sites. Partial particle agglomeration still exists, which originates from accelerated nucleation at higher $KMnO_4$ concentration and secondary agglomeration during drying. Moderate MnO_2 loading benefits energy-storage performance, whereas agglomeration blocks pores and elevates ion-diffusion resistance. By comparing 1:1 and 2:1 samples, students can directly understand how feed ratio regulates loading and dispersion, and comprehend the controlled-variable experimental ideology.

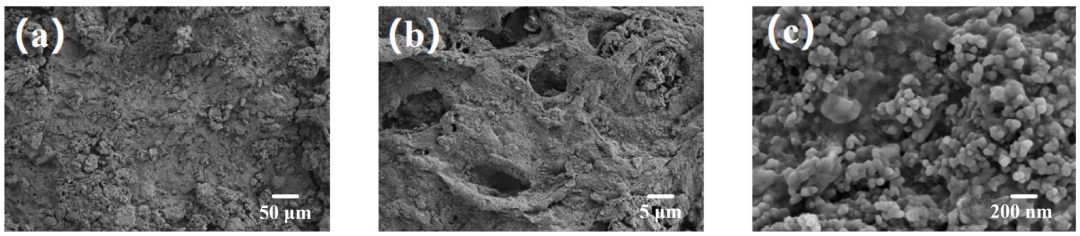

Figure 4. SEM images of RGO/MnO_2-3:1 composite at different magnifications: (a) 50 μm; (b) 5 μm; (c) 200 nm.

Table 3. Elemental composition of RGO/MnO_2-3:1 composite.

Element	Weight %	Atomic %
C	53.41	83.99
Mn	46.59	16.01
Total	100.00	100.00

Figure 4 shows characterization results of RGO/MnO_2-3:1 composite. Porous block-shaped stacking is observed at low magnification. RGO sheets are heavily wrinkled and stacked, and the surfaces as well as pore edges are covered by dense nanoparticles (**Figure 4(b)**, **Figure 4(c)**). According to **Table 3**, Mn mass fraction reaches 46.59 %, representing the highest MnO_2 loading among three groups. However, severe particle agglomeration occurs. Excessive MnO_2 supplies more

pseudocapacitive sites, yet its intrinsic poor conductivity and heavy agglomeration block internal pores, hinder electrolyte penetration and raise interfacial impedance, which is detrimental to electrochemical performance. Through this set of comparisons, students develop dialectical thinking that "higher feed dosage does not always produce better performance", and realize the existence of optimal-ratio windows for material synthesis.

3.2. Compositional Analysis of Composites

3.2.1. FTIR Spectroscopic Analysis

FTIR teaching objectives include training students to identify characteristic absorption bands, correlate peak positions with chemical-bond vibrations, and understand the scope and limitations of FTIR. Students learn to map spectral signals to material structures and improve spectrum-interpretation capabilities.

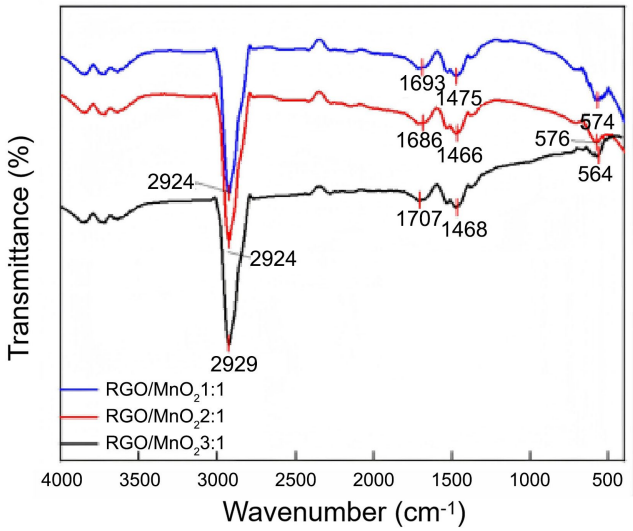

Figure 5. FTIR spectra of RGO/MnO_2-1:1, RGO/MnO_2-2:1 and RGO/MnO_2-3:1 composites.

As shown in **Figure 5**, absorption bands at 2924 - 2929 cm^{-1} correspond to C-H stretching vibrations originating from residual organic contaminants. Peaks at 1686 - 1707 cm^{-1} are assigned to C=O stretching, proving residual oxygen-containing functional groups on RGO surfaces, which serve as nucleation sites for MnO_2. Bands at 1466 - 1475 cm^{-1} originate from sp^2 C=C skeletal vibrations of graphene sheets, confirming the retention of RGO two-dimensional carbon frameworks. Characteristic bands located at 564 - 576 cm^{-1} are attributed to Mn-O/Mn-O-Mn vibrations, offering auxiliary spectral evidence for manganese-oxide formation.

Combined with EDS data in **Tables 1-3**, Mn-O absorption signals strengthen with the increase of manganese-source dosage. FTIR spectra verify that the composites possess both conductive RGO carbon frameworks and manganese-oxide active phases, laying structural foundations for the synergism of electric-double-

layer capacitance and pseudocapacitance. Nevertheless, FTIR can only identify bond types instead of precise MnO_2 crystal phases. Supplementary XRD tests are recommended for phase identification, which helps students recognize the limitations of this characterization technique.

3.2.2. Contact-Angle Measurement Analysis

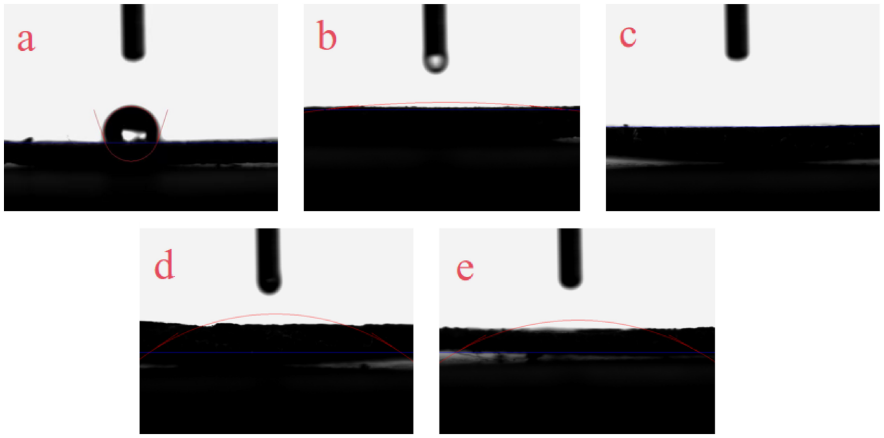

Figure 6. Contact-angle photographs: (a) nickel-foam substrate; (b) pure RGO electrode; (c) RGO/MnO_2-1:1; (d) RGO/MnO_2-2:1; (e) RGO/MnO_2-3:1 (test liquid: 1 mol/L NaCl aqueous electrolyte).

Contact-angle experiments help students intuitively understand solid-liquid interfacial wetting behavior, and establish the logical chain: "surface chemical composition/roughness determine wettability, and further affect electrochemical performance". It is emphasized that this correlation is a structural inference rather than a verified conclusion, as electrochemical tests are not performed in this study.

As displayed in **Figure 6**, liquid droplets form obvious arcs on bare nickel foam, indicating poor wettability towards aqueous electrolyte. Contact angles decrease on pure-RGO electrodes, yet the intrinsic hydrophobicity of carbon skeletons and sheet stacking still restrain electrolyte infiltration. After introducing MnO_2, droplets spread more significantly and contact angles further decline. Abundant polar Mn-O bonds and surface hydroxyl groups on MnO_2 improve surface polarity and roughness, enhancing electrode hydrophilicity. The wettability gradually improves with increasing MnO_2 loading. Superior wettability facilitates electrolyte penetration into internal pores and sufficient contact between active sites and electrolyte, lowering ion-transport resistance. Notably, this deduction is based only on interfacial characterization results. However, particle agglomeration induced by excessive MnO_2 will offset the benefits brought by improved wettability within the tested sample series.

3.2.3. BET Specific-Surface-Area and Pore-Structure Analysis

BET tests enable students to understand nitrogen-adsorption-desorption principles and the significance of specific surface area and pore structures for energy-

storage electrodes. Meanwhile, it helps break the misconception that "larger specific-surface-area always equals better performance", and promotes comprehensive evaluation combined with morphological evidence.

Table 4. Specific-surface-area parameters of different samples.

Sample	Specific surface area/$m^2 \cdot g^{-1}$	Variation trend
RGO	32.6457	Reference sample
RGO/MnO_2-1:1	49.5258	Significant increase
RGO/MnO_2-2:1	63.8202	Further increase
RGO/MnO_2-3:1	83.1689	Maximum value

As summarized in Table 4, the specific surface area of pure RGO is merely 32.6457 $m^2 \cdot g^{-1}$. The specific-surface-area values rise continuously with higher Mn-source dosage. Hydrothermally generated MnO_2 nanoparticles embed and attach on RGO sheets and interlayers, acting as spacers to mitigate tight stacking of RGO sheets and create abundant new surfaces and pores. Larger specific surface area provides more electrolyte-contact interfaces and electrochemically active sites, which favors capacitance enhancement. It should be noted that BET only reflects total specific surface area. Although the RGO/MnO_2-3:1 sample achieves the highest BET value, severe MnO_2 agglomeration observed in SEM leads to partial pore blocking. Therefore, specific surface area cannot be treated as the sole criterion for material performance. Comprehensive judgment integrating SEM morphology and contact-angle results is indispensable.

Synthesizing SEM-EDS, FTIR, contact-angle and BET results: compounding with MnO_2 alleviates RGO sheet stacking, increases specific surface area and improves aqueous-electrolyte wettability. Excess manganese-source feed ratio, however, causes serious MnO_2 agglomeration, blocks pores and raises ion-diffusion resistance. It should be noted that electrochemical performance tests are not included in this work; from the perspective of inquiry-oriented teaching experiments, the 2:1 sample exhibits optimal comprehensive structure with balanced loading, dispersion, specific surface area and wettability among the three prepared samples. The whole characterization workflow demonstrates a standard scientific-research paradigm for students: single characterization evidence has inherent limitations, and multiple mutually-validated characterizations are required to draw reliable conclusions. This practice helps students understand the necessity of multi-characterization cross-verification, cultivate critical thinking, and establish the awareness that structural superiority does not equate to superior electrochemical performance.

4. Conclusions

1) This experiment integrates Emerging-Engineering-Education concepts into inquiry-oriented comprehensive teaching. A complete experimental module of

"GO preparation-RGO reduction-hydrothermal synthesis of RGO/MnO_2 composites-multi-characterization analysis" is constructed, realizing the transformation from scientific-research subject to undergraduate teaching experiment.

2) Through this experiment, students master the basic principles and sample-preparation procedures of SEM, FTIR, contact-angle test and BET. They directly recognize how feed ratio regulates micromorphology, elemental composition, specific surface area and interfacial wettability. Students understand that MnO_2 modification relieves RGO stacking and improves electrode wettability, whereas excessive feed dosage triggers particle agglomeration and deteriorates material structures. The experiment cultivates cross-verification thinking among multiple characterizations and establishes the "preparation-condition-microstructure-material-performance" logical correlation.

3) This inquiry-based experiment changes the "cookbook-style" pattern of traditional verification experiments, fully stimulates students' research interest, and achieves the trinity educational goals of "knowledge imparting, competence cultivation and value guidance". It provides references for experimental-teaching reform of materials-related majors in engineering universities.

Acknowledgements

We acknowledge the financial support from the Tertiary Education Scientific Research Project of Guangzhou Municipal Education Bureau (No. 2026316059), the Program for Young Innovative Talents in General Universities of Guangdong Province (No. 2026KQNCX234), and the Key Project of Guangzhou Railway Polytechnic (No. GTXYZD250202).

Author Contributions

Ao Chen: Methodology, Investigation, Data analysis, Writing original draft; Hui-Yuan Zhang: Methodology, Data analysis, Verification, Supervision; Li Lian: Methodology, Supervision, Review & editing; Jie Zhang: Resources, Funding acquisition.

Conflicts of Interest

The authors declare that they have no known competing financial interests or personal relationships that could have appeared to influence the work reported in this paper.

References

[1] Charosky, G., Hassi, L., Papageorgiou, K. and Bragós, R. (2022) Developing Innovation Competences in Engineering Students: A Comparison of Two Approaches. *European Journal of Engineering Education*, **47**, 353-372. https://doi.org/10.1080/03043797.2021.1968347

[2] Phusavat, K., Ongkunaruk, P. and Anussornnitisarn, P. (2026) Gaining Insights into the Employability of University Graduates: Implications from the Students' Inputs.

Studies in Higher Education, **51**, 1571-1589.
https://doi.org/10.1080/03075079.2025.2531841

[3] Liang, Z., Chen, C., Xie, Z., Wang, Z., Cai, X., Chen, L., *et al.* (2025) The Application of Flipped Classroom Teaching Model Combining Scientific Research Expansion in the Teaching of Thoracic Surgery. *Technology and Health Care*, **33**, 755-761.
https://doi.org/10.1177/09287329241290319

[4] Almusaed, A., Almssad, A. and Najar, K. (2022) An Innovative School Design Based on a Biophilic Approach Using the Appreciative Inquiry Model: Case Study Scandinavia. *Advances in Civil Engineering*, **2022**, Article ID: 8545787.
https://doi.org/10.1155/2022/8545787

[5] Yu, J., Zhou, J., Yao, P., Xie, H., Zhang, M., Ji, M., *et al.* (2019) Antimonene Engineered Highly Deformable Freestanding Electrode with Extraordinarily Improved Energy Storage Performance. *Advanced Energy Materials*, **9**, Article ID: 1902462.
https://doi.org/10.1002/aenm.201902462

[6] Mirghni, A.A., Shuaibu, A.D., Hardianto, Y.P., Al-Qwairi, F.O., Hussain, A., Shah, S.S., *et al.* (2025) Designing Coin-Cell Supercapacitors: Combining Graphene Foam with Metal Oxide Composite Electrodes for Improved Energy Storage Performance. *FlatChem*, **50**, Article ID: 100829. https://doi.org/10.1016/j.flatc.2025.100829

[7] Xie, Q., Huang, X., Zhang, Y., Wu, S. and Zhao, P. (2018) High Performance Aqueous Symmetric Supercapacitors Based on Advanced Carbon Electrodes and Hydrophilic Poly(vinylidene fluoride) Porous Separator. *Applied Surface Science*, **443**, 412-420.
https://doi.org/10.1016/j.apsusc.2018.02.274